Surface Coordination

Deutsche Ausgabe: DOI: 10.1002/ange.201512038
Internationale Ausgabe: DOI: 10.1002/anie.201512038

Surface Coordination of Black Phosphorus for Robust Air and Water Stability

Yuetao Zhao, Huaiyu Wang, Hao Huang, Quanlan Xiao, Yanhua Xu, Zhinan Guo, Hanhan Xie, Jundong Shao, Zhengbo Sun, Weijia Han, Xue-Feng Yu,* Penghui Li, and Paul K. Chu**

Abstract: *A titanium sulfonate ligand is synthesized for surface coordination of black phosphorus (BP). In contrast to serious degradation observed from the bare BP, the BP after surface coordination exhibits excellent stability during dispersion in water and exposure to air for a long period of time, thereby significantly extending the lifetime and spurring broader application of BP.*

Atomically thin black phosphorus (BP), a new member of two-dimensional (2D) materials, has attracted increasing interest because of its unique electronic and optical properties and promising applications.[1–13] BP crystals have strong in-plane bonds and the weak van der Waals interlayer interaction enables exfoliation into few-layer BP sheets or phosphorene (single-layer BP).[14–18] As a metal-free layered semiconductor, BP has thickness-dependent band gaps varying from 0.3 eV for bulk to 2.0 eV for phosphorene.[3] Moreover, BP with high mobility and a sizeable band gap is at the electronic intersection of graphene (a zero-gap high-mobility 2D material) and semiconducting transition metal dichalcogenides (large-gap low-mobility 2D materials).[2,19–21] These fascinating properties suggest that BP is not only promising in nanoscale electronic devices,[22–26] but also suitable for near- and mid-infrared region optoelectronic applications.[27–31] Moreover, BP nanosheets possess excellent photochemical and photothermal properties with potential catalytic and biomedical applications.[11,32]

In spite of these promising properties, a fundamental obstacle hindering the application of BP is its lack of air- and water-stability.[3] It has been demonstrated that BP is very reactive to oxygen and water under ambient conditions, resulting in compositional and physical changes and consequently considerable degradation in the electronic and optical properties.[10,26,33–36] Long-term exposure of BP to humid air or water can even completely etch the materials away.[37] This poses a severe limitation to the adoption of BP in flexible electronics and photoelectronics, and its instability in water further limits potential electrochemical and biomedical applications. Therefore, much effort has been made to understand the degradation mechanism and to improve the stability of BP.[10,22,38–43] Optical microscopy and atomic force microscopy (AFM) have revealed droplet-like structures on the surface of BP upon exposure to air.[10,37,38] Consequently, capping layers have been developed to encapsulate BP sheets and enhance the air-stability of BP, but oxygen and water may enter through the interfaces causing eventual breakdown.[38] The role of oxygen and water in BP degradation has been studied recently,[42] and it has been shown that degradation of BP under ambient conditions is initiated by contact with oxygen but water does not play a primary role in the reaction. However, water is capable of removing P_xO_y from the surface and exposing P^0 to continue oxidation. Thus, preventing the reaction between BP and oxygen in air and water is crucial to enhancing the stability,[33] but accomplishing this in reality remains a great challenge.

Herein, a surface coordination strategy to enhance the stability of BP in air and water by preventing oxidization of BP is described. BP has a well-known puckered honeycomb structure in which a phosphorus atom is covalently bonded to three neighboring single-layer phosphorus atoms exposing a pair of lone pair electrons.[39] The lone pair electrons in BP can readily react with oxygen to form P_xO_y,[33] and occupation of the lone pair electrons by other elements may prevent the reaction between phosphorus and oxygen, ultimately mitigating oxidation of BP. In this study, a titanium sulfonate ligand (designated as TiL_4, L referring to the sulfonic ester group) was designed to react with BP to form TiL_4-coordinated BP (designated as TiL_4@BP) on the surface to enhance the stability in water and humid air.

The TiL_4 ligand (Figure 1a) was synthesized by a reaction between titanium tetraisopropoxide [$Ti(O^iPr)_4$] and *p*-toluenesulfonic acid in ethanol (EtOH) at 50 °C. The ^1H NMR spectra of TiL_4 in Figure 1d show a single peak at 2.2 ppm attributable to hydrogen in the $-CH_3$ group and the two double peaks at 7.2 and 7.5 ppm are associated with hydrogen atoms in the benzyl group. The ^{13}C NMR spectra (Supporting Information, Figure S1) confirm successful fabrication of TiL_4, with the peak at 20.4 ppm ascribed to carbon in $-CH_3$ and those at 125.2, 129.3, 139.2, 142.4 ppm stem from carbon atoms in the benzyl group. Transition metals, such as Ag, Au, Cu, Fe, Pd, Cr, and Ti, can be used to prepare metal–

[*] Dr. Y. Zhao, Prof. H. Wang, H. Huang, Dr. Q. Xiao, Y. Xu, Dr. Z. Guo, H. Xie, Dr. J. Shao, Dr. Z. Sun, W. Han, Prof. X.-F. Yu
Institute of Biomedicine and Biotechnology
Shenzhen Institutes of Advanced Technology
Chinese Academy of Sciences
Shenzhen 518055 (P.R. China)
E-mail: hwang1@siat.ac.cn
xf.yu@siat.ac.cn
Dr. P. Li, Prof. P. K. Chu
Department of Physics and Materials Science
City University of Hong Kong
Tat Chee Avenue, Kowloon, Hong Kong (China)
E-mail: paul.chu@cityu.edu.hk

Supporting information for this article can be found under: http://dx.doi.org/10.1002/anie.201512038.

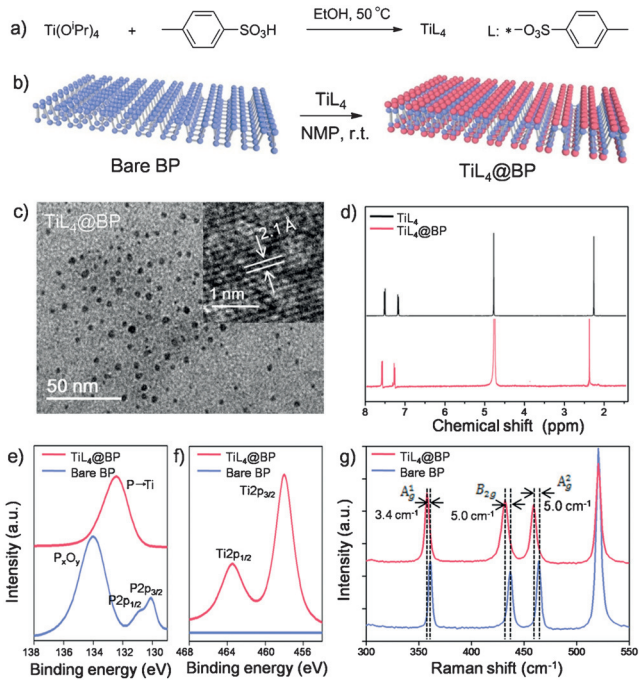

Figure 1. Fabrication and characterization of TiL_4@BP: a) Synthesis and structural formula of TiL_4; b) surface coordination of TiL_4 to BP; c) TEM image with inset HR-TEM image of TiL_4@BP; d) ^{1}H NMR spectra of TiL_4 and TiL_4@BP; e) HR-XPS spectra of P2p; f) HR-XPS spectra of Ti2p; g) Raman spectra of bare BP and TiL_4@BP.

phosphorus complexes with other patterns of phosphorus, such as tetrahedral white phosphorus, by coordinating the lone pair electrons of phosphorus in the empty orbital of the metal atoms.[44–49] Here, the TiL_4 was specifically designed to coordinate with BP because the electrophilic effect of sulfonic ester can strengthen the coordinating ability of titanium.[50]

In the next step, ultrasmall BP nanosheets (also called BP QDs) were synthesized in *N*-methyl-2-pyrrolidone (NMP) by a liquid exfoliation technique reported by our group previously,[32] and chosen as one of the BP samples in our coordination study because smaller BP sheets generally undergo faster decomposition.[33,38,42] The ultrasmall BP nanosheets were reacted with TiL_4 in NMP at room temperature for 15 h to generate the TiL_4@BP (Figure 1 b). As shown in Figure 1 c, the as-obtained TiL_4@BP nanosheets, with an average size of 3.3 nm, have good dispersability. AFM indicates that the average thickness of TiL_4@BP is about 1.6 nm (data not shown), which is the same as that previously reported from bare BP nanosheets.[32] The high-resolution transmission electron microscopy (HR-TEM) image (inset in Figure 1 c) showed lattice fringes of 0.21 nm corresponding to the (014) plane of the BP crystal.[51] The ^{1}H NMR spectra of TiL_4@BP are similar to those of TiL_4 (Figure 1 d), indicating successful coordination of TiL_4 on the BP nanosheets as well as the structure of TiL_4@BP.

High-resolution X-ray photoelectron spectroscopy (HR-XPS) is performed to assess the chemical quality of the bare BP and TiL_4@BP. The samples are prepared by drop-casting the BP dispersion onto Si/SiO_2 substrates followed by exposure to air for 72 h. As shown in Figure 1 e, the bare BP shows the $P2p_{3/2}$ and $P2p_{1/2}$ doublet at 130.1 and 130.9 eV, respectively, characteristic of crystalline BP.[32] In addition, intense oxidized phosphorus (P_xO_y) sub-bands emerged at 134.0 eV as a result of partial oxidation. This phenomenon has been observed from bare BP by XPS.[17,32] Here, the binding energy of P2p in TiL_4@BP was 132.4 eV, in agreement with the reported value of Ti–P coordination[50] and no oxidized phosphorus sub-bands could be found. Figure 1 f shows the Ti2p XPS spectra of the two samples. The $Ti2p_{1/2}$ (463.5 eV) and $Ti2p_{3/2}$ (458.0 eV) peaks were detected from TiL_4@BP, but no Ti2p peak was observed from the bare BP. XPS thus confirmed successful coordination between P and Ti in TiL_4@BP and, notably, oxidation was not observed from TiL_4@BP even after ambient exposure for 72 h.

Raman scattering was performed to characterize the bare BP and TiL_4@BP (Figure 1 g). Both TiL_4@BP and bare BP showed three prominent Raman peaks attributed to one out-of-plane phonon mode A^1_g at 359.5 cm^{-1} and two in-plane modes B_{2g} and A^2_g at 436.0 and 463.3 cm^{-1}, respectively.[3] Compared to bare BP, the A^1_g, B_{2g}, and A^2_g modes of TiL_4@BP were red-shifted by about 3.4, 5.0, and 5.0 cm^{-1}, respectively. When TiL_4 was coordinated to the BP surface, the oscillation of P atoms was hindered to some extent, thus decreasing the corresponding Raman scattering energy and producing the red-shifts of the three Raman peaks of TiL_4@BP.

To evaluate the role of Ti coordination in the BP stability, TiL_4@BP and bare BP were centrifuged from NMP, dispersed in water at a concentration of 2 ppm, and exposed to air for different time periods. The optical absorbance at each time point was monitored (Figure 2). In the beginning during dispersing, both the bare BP and TiL_4@BP showed a typical broad absorption band spanning the ultraviolet (UV) and near-infrared (NIR) regions similar to other 2D layered materials.[32] However, the absorbance intensity of the bare BP decreased significantly with dispersion time in water (Figure 2 a). After 72 h, the absorbance of the bare BP at

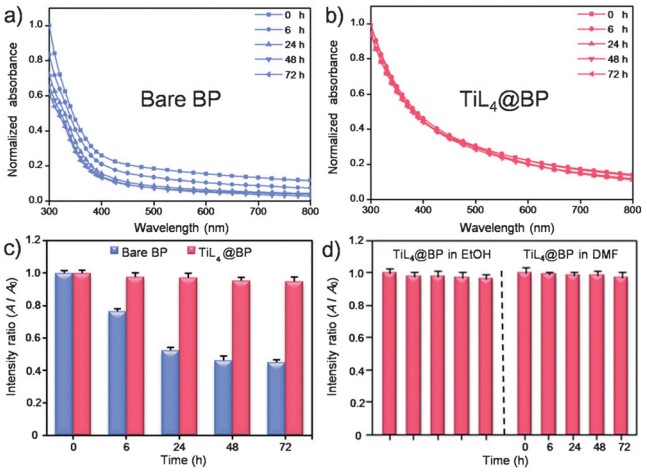

Figure 2. Stability of bare BP and TiL_4@BP in water: a) Absorption spectra of the bare BP and b) TiL_4@BP dispersed in water after exposure to air for 0, 6, 24, 48, and 72 h; c) Variation of the absorption ratios at 450 nm (A/A_0) of BP and TiL_4@BP with dispersion time in water; d) A/A_0 of TiL_4@BP with dispersion time in EtOH and DMF.

450 nm (A) decreased by 55% compared to the original value (A_0). It has been shown that degradation of BP depends on the reaction with oxygen ($P \rightarrow P_xO_y$) and water enables subsequent transformation of P_xO_y to the final anions (PO_4^{3-}).[43] This process results in quick removal of P_xO_y and continuous exposure of fresh P^0 to oxygen. The overall degradation rate of the bare BP was thus accelerated, as indicated by the reduced absorbance. In contrast, the absorbance of TiL_4@BP was maintained during dispersion in water (Figure 2b), and dispersion for 72 h in water only resulted in a 5% reduction in the absorbance intensity at 450 nm. Even when the dispersion time was increased to 1 week, only a 8% decrease in the absorbance intensity at 450 nm was observed (Figure S2). Therefore, the stability of TiL_4@BP is much better than that of the bare BP in water (Figure 2c). Additional experiments indicated that TiL_4@BP has good stablity in other common solvents, such as EtOH and *N*,*N*-dimethylformamide (DMF), under exposure to air (Figure 2d). This improvement thus enables direct use of TiL_4@BP in a variety of applications.

Photothermal agents that can convert NIR light into heat have attracted considerable attention in cancer therapy, drug/gene delivery, and tissue engineering.[52] Owing to the considerable photothermal conversion efficiency and good element biocompability, BP nanosheets are promising photothermal agents.[32] Considering that long-term exposure to the physiological environment is essential in clinical applications, the photothermal stability of TiL_4@BP dispersed in water was examined by comparing with bare BP (Figure 3). To monitor partial degradation during photothermal performance, a very low (2 ppm) concentration of TiL_4@BP and bare BP was used. The solution temperature as a function of time was studied by using the 808 nm NIR laser (1.0 $W\,c^{-2}$ at power density) as the light source. In the beginning during water dispersion, the solution temperature of the bare BP increased by 10.5 °C after irradiation for 10 min, and it was accompanied by severe degradation of the photothermal performance with time. After 72 h, the solution temperature of the bare BP increased by 3.1 °C with 10 min irradiation. In contrast, the photothermal performance of TiL_4@BP was much better. After 72 h, the temperature of the TiL_4@BP solution increased by 9.6 °C with 10 min irradiation, and it was close to the original value of 10.5 °C. The slight decrease of temperature-rise is probably due to the slight aggregation of the sample. The difference in the photothermal performance between the bare BP and TiL_4@BP is consistent with the optical absorbance shown in Figure 2. It should be noted that the TiL_4 molecules showed neither obvious NIR absorption nor photothermal characteristics (Figure S3). Furthermore, biological experiments were performed and excellent biocompatibility with different cells was observed with TiL_4@BP (Figure S4). When illuminated by the 808 nm laser, the TiL_4@BP exhibited good photothermal effect, as evidenced by death of cancer cells (Figure S5). By performing simple TiL_4-coordination, BP can maintain the photothermal performance in a physiological environment, thereby boding well for biomedical application of the materials.

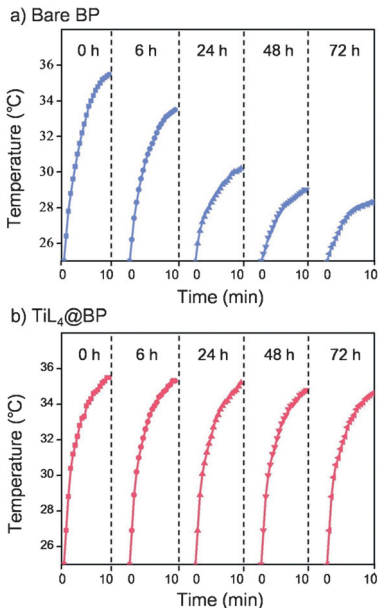

Figure 3. Photothermal heating curves of a) Bare BP and b) TiL_4@BP dispersed in water after exposure to air for 0, 6, 24, 48, and 72 h using the 808 nm laser as the irradiation source.

To further assess the stability of TiL_4@BP with different sizes, micro-sized BP sheets were synthesized by the liquid exfoliation method reported by our group previously[31] and employing the TiL_4 coordination as described above. The TiL_4@BP sheets and bare BP sheets (control) were dropped onto Si/SiO_2 substrates and kept in air at a relative humidity of 95% at room temperature for different time durations (Figure 4). Figures 4a and 4b, respectively, present the optical images of the freshly prepared bare BP and TiL_4@BP sheets and after exposure to humid air for 12 and 24 h. With regard to the bare BP, the surface appeared optically flat during initial exposure and the surrounding Si/SiO_2 substrate is featureless in the optical micrograph. After exposure for 12 h, small water droplets are observed from the sheet surface, and after exposure for 24 h the droplets become larger and denser. Meanwhile, the color of the sheet changed probably because it becomes thinner.[38,53] It is evident from the AFM images (Figure 4c) that the sheet surface was roughened by the droplets. These findings are consistent with the previously reported morphological changes on BP sheets in air.[39,42] In comparison, the TiL_4@BP sheet was almost unchanged after exposure to humid air for 24 h. The AFM images in Figure 4d show that the TiL_4@BP sheet was smoother than the bare BP sheet after 24 h. Both optical microscopy and AFM provide direct evidence about the effectiveness of TiL_4-coordination in protecting BP from oxidation in air with a relative humidity as high as 95%. BP sheets have potential applications in electronics because of unique characteristics, including the anisotropic nature,[2,3,22,24,26] layer-dependent direct band gap energy,[5,11] and 2D-layered hinge-like structure.[8] In theory, the surface modification strategy described here should not influence these characteristics, and the enhanced stability can in fact be exploited to expedite the use of the materials in different applications.

In conclusion, a titanium sulfonate ligand (TiL_4) was synthesized to coordinate with BP to form TiL_4@BP. The P–Ti

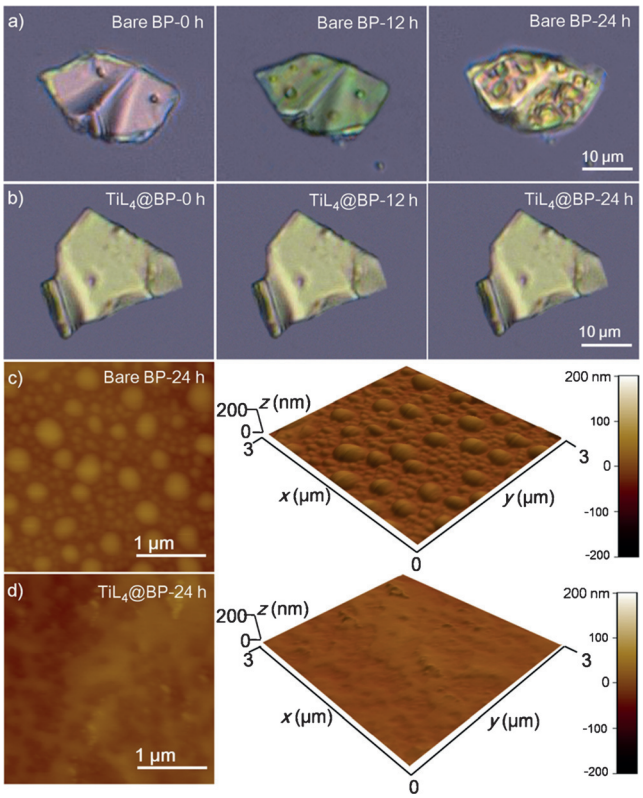

Figure 4. Stability of micro-sized bare BP and TiL_4@BP sheets in air with a relative humidity of 95%: Optical images of a) bare BP and b) TiL_4@BP sheets on Si/SiO_2 and exposed to the humid air at room temperature for 0 (left), 12 (middle), and 24 h (right). Selected AFM scans of c) BP and d) TiL_4@BP sheet after exposure to the humid air for 24 h.

coordination occupies the lone pair electrons of phosphorus, preventing oxidation of BP in air and water. The stability of the bare BP and TiL_4@BP under different conditions was studied systematically in terms of the structure and performance. In contrast to serious degradation observed from the bare BP, the TiL_4@BP nanosheet exhibited excellent stability during long-term dispersion in water as well as exposure to air, and degradation in the optical absorbance and photothermal performance was minimal. Optical microscopy and AFM demonstrated that TiL_4-coordination protects BP from oxidation in air with a relative humidity as high as 95%. Our findings provide a simple and efficient strategy to enhance the stability of BP against oxidation and degradation. The TiL_4@BP with excellent stability in air and water has many potential applications in nanoelectronics, optoelectronics, and biomedicine.

Acknowledgements

This work was supported by the National Natural Science Foundation of China (NSFC) Nos. 51372175 and 31470044, Leading Talents of Guangdong Province Program No. 00201520, Shenzhen Peacock Program No. 110811003586331, Shenzhen Science and Technology Research Funding Nos. JCYJ20140417113430608 and JCYJ20150401145529017, as well as City University of Hong Kong Applied Research Grant (ARG) No. 9667104.

Keywords: black phosphorus · degradation · oxidation · phosphorenes · stability

How to cite: *Angew. Chem. Int. Ed.* **2016**, *55*, 5003–5007
Angew. Chem. **2016**, *128*, 5087–5091

[1] H. O. Churchill, P. Jarillo-Herrero, *Nat. Nanotechnol.* **2014**, *9*, 330.
[2] L. Li, Y. Yu, G. J. Ye, Q. Ge, X. Ou, H. Wu, D. Feng, X. H. Chen, Y. Zhang, *Nat. Nanotechnol.* **2014**, *9*, 372.
[3] H. Liu, A. T. Neal, Z. Zhu, Z. Luo, X. F. Xu, D. Tománek, P. D. Ye, *ACS Nano* **2014**, *8*, 4033.
[4] A. S. Rodin, A. Carvalho, A. H. Castro Neto, *Phys. Rev. Lett.* **2014**, *112*, 176801.
[5] J. S. Qiao, X. H. Kong, Z. X. Hu, F. Yang, W. Ji, *Nat. Commun.* **2014**, *5*, 4475.
[6] D. Xiang, C. Han, J. Wu, S. Zhong, Y. Y. Liu, J. D. Lin, X. A. Zhang, W. P. Hu, B. Özyilmaz, A. H. Castro Neto, A. T. Shen Wee, W. Chen, *Nat. Commun.* **2015**, *6*, 6485.
[7] X. M. Wang, A. M. Jones, K. L. Seyler, V. Tran, Y. C. Jia, H. Zhao, H. Wang, L. Yang, X. D. Xu, F. N. Xia, *Nat. Nanotechnol.* **2015**, *10*, 517.
[8] G. Z. Qin, Q. B. Yan, Z. Z. Qin, S. Y. Yue, H. J. Cui, Q. R. Zheng, G. Su, *Sci. Rep.* **2014**, *4*, 6946.
[9] J. X. Wu, N. N. Mao, L. N. Xie, H. Xu, J. Zhang, *Angew. Chem. Int. Ed.* **2015**, *54*, 2366; *Angew. Chem.* **2015**, *127*, 2396.
[10] R. A. Doganov, E. C. T. O'Farrell, S. P. Koenig, Y. T. Yeo, A. Ziletti, A. Carvalho, D. K. Campbell, D. F. Coker, K. Watanabe, T. Taniguchi, A. H. Castro Neto, B. Özyilmaz, *Nat. Commun.* **2015**, *6*, 6647.
[11] S. Zhang, J. Yang, R. J. Xu, F. Wang, W. F. Li, M. Ghufran, Y. W. Zhang, Z. F. Yu, G. Zhang, Q. H. Qin, Y. R. Lu, *ACS Nano* **2014**, *8*, 9590.
[12] S. Appalakondaiah, G. Vaitheeswaran, S. Lebegue, N. E. Christensen, A. Svane, *Phys. Rev. B* **2012**, *86*, 035105.
[13] Y. W. Wang, G. H. Huang, H. R. Mu, S. H. Lin, J. Z. Chen, S. Xiao, Q. L. Bao, *Appl. Phys. Lett.* **2015**, *107*, 091905.
[14] J. R. Brent, N. Savjani, E. A. Lewis, S. J. Haigh, D. J. Lewis, P. Óbrien, *Chem. Commun.* **2014**, *50*, 13338.
[15] P. Yasaei, B. Kumar, T. Foroozan, C. H. Wang, M. Asadi, D. Tuschel, J. E. Indacochea, R. F. Klie, A. Salehi-Khojin, *Adv. Mater.* **2015**, *27*, 1887.
[16] X. Zhang, H. M. Xie, Z. D. Liu, C. L. Tan, Z. M. Luo, H. Li, J. D. Lin, L. Q. Sun, W. Chen, Z. C. Xu, L. H. Xie, W. Huang, H. Zhang, *Angew. Chem. Int. Ed.* **2015**, *54*, 3653; *Angew. Chem.* **2015**, *127*, 3724.
[17] J. Kang, J. D. Wood, S. A. Wells, J. H. Lee, X. L. Liu, K. S. Chen, M. C. Hersam, *ACS Nano* **2015**, *9*, 3596.
[18] A. H. Woomer, T. W. Farnsworth, J. Hu, R. A. Wells, C. L. Donley, S. C. Warren, *ACS Nano* **2015**, *9*, 8869.
[19] A. K. Geim, K. S. Novoselov, *Nat. Mater.* **2007**, *6*, 183.
[20] J. L. Wang, X. M. Zou, X. H. Xiao, L. Xu, C. L. Wang, C. Z. Jiang, J. C. Ho, T. Wang, J. C. Li, L. Liao, *Small* **2015**, *11*, 208.
[21] H. L. Wang, X. W. Zhang, J. H. Meng, Z. G. Yin, X. Liu, Y. J. Zhao, L. Q. Zhang, *Small* **2015**, *11*, 1542.
[22] F. N. Xia, H. Wang, Y. C. Jia, *Nat. Commun.* **2014**, *5*, 4458.
[23] D. J. Perello, S. H. Chae, S. Song, Y. H. Lee, *Nat. Commun.* **2015**, *6*, 7809.
[24] R. X. Fei, L. Yang, *Nano Lett.* **2014**, *14*, 2884.
[25] J. Y. Jia, S. K. Jang, S. Lai, J. Xu, Y. J. Choi, J. H. Park, S. J. Lee, *ACS Nano* **2015**, *9*, 8729.

[26] M. Buscema, D. J. Groenendijk, S. I. Blanter, G. A. Steele, H. S. J. van der Zant, A. Castellanos-Gomez, *Nano Lett.* **2014**, *14*, 3347.
[27] M. Engel, M. Steiner, P. Avouris, *Nano Lett.* **2014**, *14*, 6414.
[28] H. Wang, X. M. Wang, F. N. Xia, L. H. Wang, H. Jiang, Q. F. Xia, M. L. Chin, M. Dubey, S. J. Han, *Nano Lett.* **2014**, *14*, 6424.
[29] T. Low, A. S. Rodin, A. Carvalho, Y. J. Jiang, H. Wang, F. N. Xia, A. H. Castro Neto, *Phys. Rev. B* **2014**, *90*, 075434.
[30] H. R. Mu, S. H. Lin, Z. C. Wang, S. Xiao, P. F. Li, Y. Chen, H. Zhang, H. F. Bao, S. P. Lau, C. X. Pan, D. Y. Fan, Q. L. Bao, *Adv. Opt. Mater.* **2015**, *3*, 1447.
[31] Z. N. Guo, H, Zhang, S. B. Lu, Z. T. Wang, S. Y. Tang, J. D. Shao, Z. B. Zun, H. H. Xie, H. Y. Wang, X. F. Yu, P. K. Chu, *Adv. Funct. Mater.* **2015**, *25*, 6996.
[32] Z. B. Sun, H. H. Xie, S. Y. Tang, X. F. Yu, Z. N. Guo, J. D. Shao, H. Zhang, H. Huang, H. Y. Wang, P. K. Chu, *Angew. Chem. Int. Ed.* **2015**, *54*, 11526; *Angew. Chem.* **2015**, *127*, 11688.
[33] A. Favron, E. Gaufrès, F. Fossard, A. L. P. L′Heureux, N. Y. W. Tang, P. L. Lévesque, A. Loiseau, R. Leonelli, S. Francoeur, R. Martel, *Nat. Mater.* **2015**, *14*, 826.
[34] J. S. Kim, Y. Liu, W. Zhu, S. Kim, D. Wu, L. Tao, A. Dodabalapur, K. Lai, D. Akinwande, *Sci. Rep.* **2015**, *5*, 8989.
[35] A. Avsar, I. J. Vera-Marun, J. Y. Tan, K. Watanabe, T. Taniguchi, A. H. Castro Neto, B. Özyilmaz, *ACS Nano* **2015**, *9*, 4138.
[36] J. D. Wood, S. A. Wells, D. Jariwala, K. S. Chen, E. K. Cho, V. K. Sangwan, X. L. Liu, L. J. Lauhon, T. J. Marks, M. C. Hersam, *Nano Lett.* **2014**, *14*, 6964.
[37] A. Castellanos-Gomez, L. Vicarelli, E. Prada, J. O. Island, K. L. Narasimha-Acharya, S. I. Blanter, D. J. Groenendijk, M. Buscema, G. A. Steele, J. V. Alvarez, H. W. Zandbergen, J. J. Palacios, H. S. J. van der Zant, *2D Mater.* **2014**, *1*, 025001.
[38] J. O. Island, G. A. Steele, H. S. van der Zant, A. Castellanos-Gomez, *2D Mater.* **2015**, *2*, 011002.
[39] A. Ziletti, A. Carvalho, D. K. Campbell, D. F. Coker, A. H. Castro Neto, *Phys. Rev. Lett.* **2015**, *114*, 046801.
[40] A. Ziletti, A. Carvalho, P. E. Trevisanutto, K. Campbell, F. Coker, A. H. Castro Neto, *Phys. Rev. B* **2015**, *91*, 085407.
[41] J. P. Lu, J. Wu, A. Carvalho, A. Ziletti, H. W. Liu, J. Y. Tan, Y. F. Chen, A. H. Castro Neto, B. Özyilmaz, C. H. Sow, *ACS Nano* **2015**, *9*, 10411.
[42] Y. Huang, K. He, S. Bliznakov, E. Sutter, F. Meng, D. Su, T. Sutter, *Con-mat.mtrl-sci* arXiv: 1511.09201.
[43] G. X. Wang, W. J. Slough, R. Pandey, S. P. Karna, *Con-mat.mtrl-sci* arXiv: 1508.07461.
[44] I. Krossing, *J. Am. Chem. Soc.* **2001**, *123*, 4603.
[45] L. C. Forfar, T. J. Clark, M. Green, S. M. Mansell, C. A. Russell, R. A. Sangurama *th*, J. M. Slattery, *Chem. Commun.* **2012**, 48, 1970.
[46] G. Santiso-Quiñones, A. Reisinger, J. Slattery, I. Krossing, *Chem. Commun.* **2007**, *43*, 5046.
[47] X. J. Kuang, X. Q. Wang, G. B. Liu, *Transition Met. Chem.* **2011**, *36*, 45.
[48] R. M. Kagirov, A. V. Voloshin, M. K. Kadirov, I. R. Nizameev, O. G. Sinyashin, D. G. Yakhvarov, *Mendeleev Commun.* **2011**, *21*, 201.
[49] X. J. Kuang, X. Q. Wang, G. B. Liu, *Phys. B* **2010**, *405*, 3328.
[50] S. T. Huang, R. R. Tang, B. Li, A. L. Ding, *Chin. J. Appl. Chem.* **1988**, *5*, 30.
[51] R. Hultgren, N. S. Gingrich, B. E. Warren, *J. Chem. Phys.* **1935**, *3*, 351.
[52] L. Cheng, C. Wang, L. Z. Feng, K. Yang, Z. Liu, *Chem. Rev.* **2014**, *114*, 10869.
[53] G. Rubio-Bollinger, R. Guerrero, D. P. de Lara, J. Quereda, L. Vaquero-Garzon, L. Vaquero-Garzon, N. Agraït, R. Bratschitsch, A. Castellanos-Gomez, *Electronics* **2015**, *4*, 847.

Received: December 31, 2015
Revised: January 31, 2016
Published online: March 15, 2016

